Dorsal and ventral cortices are coupled by cross-frequency interactions during working memory

Popov, Tzvetan; Jensen, Ole; Schoffelen, Jan-Mathijs

[Link to publication on Research at Birmingham portal](#)

Dorsal and ventral cortices are coupled by cross-frequency interactions during working memory

Tzvetan Popov[1], Ole Jensen[2,3], Jan-Mathijs Schoffelen[2]

Author's affiliations:

1- Department of Psychology, Universtität Konstanz, Germany

2- Radboud University Nijmegen, Donders Institute for Brain, Cognition and Behaviour, Center for Cognitive Neuroimaging, The Netherlands

3- School of Psychology, University of Birmingham, Hills Building, Birmingham B15 2TT

Corresponding author: Jan-Mathijs Schoffelen

e-mail: jan.schoffelen@donders.ru.nl

Corresponding address: Kapitelweg 29, 6525 EN Nijmegen, P.O. Box 91101, 6500 HB

Nijmegen, The Netherlands

Tel. +31 (0)24 3614793

1

Abstract

Oscillatory activity in the alpha and gamma bands is considered key in shaping functional brain architecture. Power increases in the high-frequency gamma band are typically reported in parallel to decreases in the low-frequency alpha band. However, their functional significance and in particular their interactions are not well understood. The present study shows that, in the context of an N-back working memory task, alpha power decreases in the dorsal visual stream were related to gamma power increase in early visual areas. Granger causality analysis revealed directed interregional interactions from dorsal to ventral stream areas, in accordance with task demands. Present results reveal a robust, behaviorally relevant, and architectonically decisive power-to-power relationship between alpha and gamma activity. This relationship suggests that anatomically distant power fluctuations in oscillatory activity can link cerebral network dynamics on trial-by-trial basis during cognitive operations such as working memory.

2

Introduction

Rhythmic neuronal activity is a ubiquitous phenomenon that underlies the spectral components that can be readily observed in electrophysiological recordings. In recent decades a large body of empirical evidence has been collected that provides a link between oscillatory activity in specific frequency bands and their functional role in cognition. For instance, amplitude fluctuations in alpha oscillatory activity (8-14Hz) have been found to be related to cognitive processes such as perception, attention, and memory (Gevins et al., 1997; Cooper et al., 2003; Klimesch et al., 2007; Jensen and Mazaheri, 2010; Saalmann et al., 2012; van Kerkoerle et al., 2014; Bastos et al., 2015; Michalareas et al., 2016; Popov et al., 2017). Specifically, decreases in alpha amplitude have been proposed to index engagement of a cortical area, whereas increases mark reduced processing capabilities. This has been demonstrated in the visual (Adrian and Matthews, 1934; Foxe et al., 1998), sensorimotor (Haegens et al., 2010; Haegens et al., 2011; van Ede et al., 2014), and auditory (Weisz et al., 2011; Mazaheri et al., 2014) domains, suggesting an overarching principle for effective neuronal resource allocation in a regionally specific manner.

Faster rhythms (gamma oscillations, >30Hz), on the other hand, have been frequently linked to coherent stimulus processing (Tallon-Baudry and Bertrand, 1999; Fries, 2005), attention (Bauer et al., 2014; Marshall et al., 2015a; Marshall et al., 2015b), and working memory (Tallon-Baudry et al., 1998; Roux et al., 2012). It is well known that fast and slow rhythms frequently co-occur and that they are often co-modulated (or anti-modulated) as a consequence of an experimental manipulation. This has led to the idea that dynamic interactions between slow and fast oscillatory activity might be a key mechanism shaping functional interactions in cortical networks (Buzsaki and Draguhn, 2004; Canolty and Knight, 2010; Lisman and Jensen, 2013).

One possible mechanism by which fast rhythms could interact with slower rhythms is by means of phase-amplitude coupling (PAC) (Jensen and Colgin, 2007; Canolty and Knight, 2010), where slow oscillations phasically modulate the amplitude of faster rhythms. PAC has been identified in a variety of species, including rodents (Tort et al., 2009; Tort et al., 2010), nonhuman primates (Whittingstall and Logothetis, 2009; Spaak et al., 2012), and humans (Canolty and Knight, 2010). Moreover, PAC has been demonstrated during cognitive

3

operations such as item-context binding (Tort et al., 2009), spatial navigation and decision making (Tort et al., 2008), working (Axmacher et al., 2010; Leszczynski et al., 2015) and episodic memory (Staudigl and Hanslmayr, 2013; Park et al., 2016), sleep (Staresina et al., 2015), and resting conditions (Florin and Baillet, 2015) and in a variety of clinical conditions such as Parkinson's disease (van Wijk et al., 2016), schizophrenia (Allen et al., 2011; Kirihara et al., 2012; Popov and Popova, 2015), autism (Berman et al., 2015), and affective disorders (Miskovic et al., 2011).

Another view of the relationship between slow and fast oscillatory activity comes from recent work investigating the network properties of directed oscillatory coupling [e.g. Granger causality (GC)] between brain regions in humans and non-human primates. Long-range inter-regional gamma synchronization has been shown to reflect feed-forward interactions within the visual cortical hierarchy, whereas slower alpha-beta synchronization reflects feedback interactions (van Kerkoerle et al., 2014; Bastos et al., 2015; Michalareas et al., 2016). These findings are in line with generic anatomical connection profiles between cortical layers, both within and between cortical areas, and with the cortical-layer-specific distribution of different neuronal rhythms.

A third type of interaction could involve a relationship between the oscillations' amplitudes. In contrast to the PAC and GC measures, this type of functional interaction does not require a strict relationship of the oscillations' phase between brain areas. In fact, a number of studies have reported stimulus-induced increases in gamma band activity with a concomitant decrease in alpha-beta power [e.g. (Schoffelen et al., 2005; Hoogenboom et al., 2006; Swettenham et al., 2009; Hoogenboom et al., 2010; Muthukumaraswamy and Singh, 2013; Perry et al., 2013; Bauer et al., 2014; Kujala et al., 2015; Michalareas et al., 2016)]. These empirical observations suggest a negative correlation between the task-induced amplitude modulations of slow versus fast rhythms.

Yet a functionally relevant mechanistic relationship between low- and high-frequency oscillatory activity, where a temporary increase in low-frequency power leads to a temporary reduction in high-frequency power, would suggest a negative correlation within trials. Reports of this nature are far less frequent in the literature (de Lange et al., 2008; Park

4

et al., 2011; Popov et al., 2017; Wang et al., 2017), which may be a consequence of the fact that single-trial estimates of oscillatory amplitudes typically have low signal-to-noise ratio, in particular when estimated from non-invasively recorded data.

The present study leveraged the availability of a large number of subjects (n = 83), analyzing MEG data from a publicly available dataset. Participants performed a visual working memory (WM) N-back task, which reliably induces modulations in both alpha and gamma activity (Roux and Uhlhaas, 2014). Thus, these data are well suited to investigate the relationship between WM-load-dependent local changes in low- and high-frequency oscillatory activity, both across time within trials and across subjects. We hypothesized that WM demands would manifest as power-power interactions, where reductions in alpha activity would be associated with a spatially specific power increase in gamma activity. Second, these power fluctuations should be related to behavioral performance both within and between trials. Third, "top-down" influence within key network nodes should be reflected in low-frequency activity, whereas "bottom-up" communication should be evident in high-frequency activity.

Material and methods

Participants and experimental procedures

Publicly available data provided by the human connectome consortium (www.humanconnectome.org) were analyzed. Eighty-three subjects (37 female and 46 male, mean age 28.5 years, range 22-35) participated in the experiment. Most were right-handed as measured with the Edinburgh Handedness Inventory with an mean lateralization quotient of 65% and SD = 44% (Oldfield, 1971). Participants gave written informed consent for participation in accordance with the Declaration of Helsinki. In two runs, participants performed an N-back WM paradigm, memorizing pictures of faces and tools. Subjects were presented with 16 blocks per run of 0-back and 2-back trials and were asked to indicate match and no-match responses via button press with their right index and right middle finger, respectively (Figure 1). An initial cue presented for 2500 ms signaled the beginning of either a 0- or a 2-back block. After this, a serial presentation of face or tool stimuli displayed for 2000 ms was intermixed with an inter-stimulus intervals (ISI) of 500 ms. Participants were asked to respond as fast as possible via button press after the presentation of each stimulus. Responses had to take place within the stimulus presentation window. Following a

1   fixation interval of 500 ms, the next trial was presented.

2

3   *Data acquisition and analysis*

4   Data were recorded using a whole-head 248-channel magnetometer system (MAGNES 3600

5   WH, 4D Neuroimaging, San Diego, CA) with subjects supine. Data were continuously

6   recorded with a sampling rate of 2034.5101 Hz and a bandwidth of DC-400Hz. Digitization of

7   each head shape and of the locations of the fiducial coils was accomplished with a Polhemus

8   3Space Fasttrak system. The WM task was a part of a 3-hour session, where both task and

9   resting-state MEG data were collected. Participants performed a sequence of tasks,

10   described in detail in the reference manual provided by the human connectome consortium

11   (http://www.humanconnectome.org/documentation/S500/index.html). Just prior to the N-

12   back paradigm the participant underwent three runs of approximately 6 minutes of resting-

13   state MEG recording.

14

15   The analysis described below was performed on the 'minimally preprocessed' data that were

16   downloaded from the human connectome database. In brief, epochs lasting from 1.5 s

17   before to 2.5 s after each picture's onset had been extracted from the continuous recording.

18   Epochs containing superconducting quantum interference device (SQUID) jumps, bad

19   sensors, or bad segments, defined as excessive signal amplitude changes > ~10^{-12}T, were

20   excluded from further processing. Eye-movement-related signals and cardiac signals had

21   been identified with independent component analysis (ICA) (Jung et al., 2001) and projected

22   out of the data. All data was analysed using custom scripts in MATLAB and the FieldTrip

23   toolbox (Oostenveld et al., 2011).

24

25   *Spectral analysis*

26   For each epoch, spectral analysis was performed using a windowed Fast Fourier Transform

27   (FFT). For frequencies below 40 Hz, we used a 500 ms sliding window (sliding in steps of 50

28   ms) multiplied by a Hanning taper, achieving an effective frequency resolution of ~2 Hz. For

29   high frequency activity (>40 Hz), we used multitapers (Mitra and Pesaran, 1999). Eleven

30   orthogonal Slepian tapers were used, resulting in a spectral smoothing of $\pm$ 10Hz.

31

32   *Source level analysis*

Source reconstruction of oscillatory activity was performed using the dynamic imaging of coherent sources (DICS) algorithm (Gross et al., 2001). This algorithm uses the sensor-level cross-spectral density matrix and a set of location-specific forward models to construct a set of spatial filters optimized for a given frequency at the specific locations. The data of both conditions were used for the spatial filter computation, which were subsequently used to compute the pattern of oscillatory activity for each condition separately. A realistic, single-shell brain model (Nolte, 2003) was constructed based on the individual anatomical MRI as implemented in FieldTrip. Forward models were computed using the anatomical information provided in the database, consisting of a subject-specific, realistically shaped single shell volume conduction model and a 3-dimensional grid of dipole locations with equidistant positions in normalized MNI-space (spacing of 8 mm).

For a set of predefined locations, we reconstructed time courses of neuronal activity using a linearly constrained minimum variance (LCMV) beamformer (Van Veen et al., 1997). These locations were identified by contrasting source-reconstructed power estimates of alpha and gamma activity for the 2- vs. 0-back conditions resulting in differential effects in primary visual areas (V1), intra-parietal sulcus (IPS), and fusiform gyrus (FF) (see Figure 1). Local maxima were identified in right FF [MNI coordinates: 55 -58 -12], right intraparietal sulcus IPS [MNI coordinates: 34 -76 28], and primary visual cortex V1 [MNI coordinates: 4 -80 8]. Spatial filters were estimated based on the unfiltered data covariance matrix for all trials and forward models of the locations of interest. Subsequently, these filters were multiplied by the data in order to obtain 'virtual channel' time series at the respective locations.

Correlation analyses
Brain-behavior relationships
The relationship between behavioral measures (average reaction times, RT, or RT differences) and trial-averaged neural data were computed as Spearman's rank correlation across participants. This relationship was computed for each sensor, time, and frequency bin, and statistical inference was done using cluster-based permutation tests (see below). Within-subject Spearman correlations across trials, using single trial RTs and neural data at sensor level, were also computed.

7

Cross-frequency power-power correlations

In order to assess cross-frequency power-power correlations, Spearman correlations characterized cross-frequency alpha-gamma power-power relationships. At the sensor level, stimulus-induced gamma activity (60-80Hz) in visual areas was correlated with the estimated power at each sensor, time point, and frequency bin (up to 40 Hz). Gamma power was quantified as a single value per participant, computed as the mean over occipito-parietal sensors, frequencies, and time points. The inclusion criteria for sensors, time points, and frequencies were based on the condition differences (2-back vs. 0-back) in gamma activity (see Figure 1A). In addition, trial-by-trial relationships were evaluated at source level. First, generators of alpha and gamma oscillatory signals were determined by a spatial filtering algorithm (see below) ,and time courses of neuronal activity at these locations were extracted. Next, within participants, two sets of high and low alpha trials per location were identified on the basis of a median split on alpha power. Finally, the null hypothesis of no group differences in gamma amplitudes in high and low alpha trials was evaluated using the cluster-based permutation framework.

Granger causality analysis and parcellation of source-reconstructed activity

Spectrally resolved Granger causality (GC) analysis (Granger, 1969; Ding et al., 2006) was used to dissociate potential directionality in inter-nodal communication. Briefly, GC represents the result of a model comparison where the predictive strength of past values of time series *x* predicting the future behavior of time series *x* (a univariate auto-regressive model) is evaluated against the past values of time series *x* and another time series *y* (a bivariate auto-regressive model) predicting the future behavior of time series *x*. Initially formulated in the time domain, GC can also be estimated in the frequency domain (Geweke, 1982; Kaminski et al., 2001; Chen et al., 2006) [see for detailed review (Bastos and Schoffelen, 2015) and (Ding et al., 2006)], which requires the estimation of the spectral transfer matrix between a set of signals.

A whole-cortex all-to-all GC analysis was performed. In a first step, the dimensionality of the data was reduced by applying an atlas-based parcellation scheme (Glasser et al., 2016). This atlas discretizes the neocortex into 180 parcels per hemisphere, which can be further grouped into 22 modality-specific areas, e.g. auditory, somatosensory, visual, task-

positive, and task-negative. Following procedures similar to those of (Schoffelen et al., 2017), single-dipole-specific spatial filters were concatenated across vertices comprising a parcel, yielding a set of 22 multivariate time courses of activity per hemisphere. For each parcel, the spatial components explaining 95% of the variance within the corresponding parcel were selected. Out of these preselected components, only the first (largest) component was considered for further analysis. This step is motivated by the fact that differences in local dipole orientations preclude averaging over a set of components within a parcel, potentially leading to cancelation of effects. For comparability purposes, source power analysis of alpha and gamma activity was re-computed as described above followed by whole-brain (all to all parcels) conditional GC analysis. Parcel time series were re-segmented to include 1 to 2 seconds post-stimulus-onset (the post-stimulus task window). For each trial, Fourier coefficients were computed for the entire spectrum up to the Nyquist frequency. Non-parametric matrix factorization of the cross-spectral density matrix (Wilson, 1972; Dhamala et al., 2008) estimated the spectral transfer matrix. For a given pair of locations, GC was computed conditional on the rest of locations, similar to the procedures applied in (Wen et al., 2013) and (Bastos et al., 2015). In addition, GC influences were computed twice: once on the original and once on the time-reversed time series. The latter strategy proposed by (Haufe et al., 2013; Winkler et al., 2015) accounts for the presence of so-called weak asymmetries as a possible interpretational confound, contributing to an apparent dominant directional drive between two areas. Briefly, as opposed to strong asymmetries, which are caused by actual time-lagged relations between signals, weak asymmetries are the consequence of differences in univariate signal properties (for instance, the local signal-to-noise ratio). Time reversal of the signals does not affect these univariate signal properties, whereas it should reverse the dominant direction of interaction. In other words, if similar patterns of GC are observed after the time reversal, these are most likely artificial, whereas a reversal of the direction of the asymmetry implies true time-lagged, thus directed relationships. Only relationships surviving the contrast *[forward minus backward vs. foraward$_{flip}$ minus backward$_{flip}$]* are presented and evaluated in this report.

Statistical analysis

Inferential statistical evaluation was carried out by non-parametric permutation tests (Maris and Oostenveld, 2007). A cluster-based approach, clustering across space, time points, and frequency (wherever appropriate) controlled for multiple comparisons, using

9

1   1000 permutations and an alpha threshold of 0.025.

2

Results

The present study evaluated publicly available neuromagnetic data from human participants performing an alternating WM task. In a block design, participants performed either 0 or 2-back task. Each block began with a cue indicating the WM load condition for 2.5 s followed by presentation of face or tool stimuli. Stimulus duration was 2 s separated by a 0.5 s interstimulus interval (offset to onset) during which participants were asked to provide a response (Figure 1).


Figure 1: Experimental task. A- At the beginning of the 0-back block, participants are presented with a target face X. On subsequent trials different faces are presented. After each face, participants indicate via button press whether the presented stimulus matches the target stimulus. Responses had to occur within 500 ms after the stimulus offset. B- 2-back blocks were signaled by a presentation of "2-back" for 2500 ms. Participants indicated whether the presented stimulus matched the stimulus two trials earlier. Responses had to occur in 500 ms after stimulus offset.

Alpha-beta and gamma activity in object-selective areas scale with working memory load

As a first step, we evaluated the effect of WM load on the time-frequency response of the brain. Compared to the 0-back condition, the 2-back condition was associated with an amplitude decrease in alpha-beta power (8-15Hz) and an increase in gamma power (60-80 Hz) ($p < 0.01$, non-parametric randomization)(Figure 2A). Sensor-level effects were widespread, with the largest difference at occipital sensors (Figure 2B). Source reconstruction of these effects, however, suggests different cortical generators of the observed topographies (Figure 2C). Alpha-beta condition differences

1 were strongest in bilateral fusiform gyri and right intra parietal sulcus (IPS). In contrast,

2 gamma effects were strongest in early visual areas around the primary visual cortex

3 (V1). The chosen threshold of 80 % of maximum is arbitrary, and source extent should

4 be interpreted with caution. The largest observed power difference occur on average

5 at peak minimum of 800 ms for alpha and peak maximum of 650 ms for gamma

6 activity. Button responses following stimulus presentation occurred on average at 631

7 ms for 0-back (min/max = 394/1053 ms, SD = 128 ms) and 827 ms for 2-back (min/max

8 = 511/1161 ms, SD = 131 ms).

9
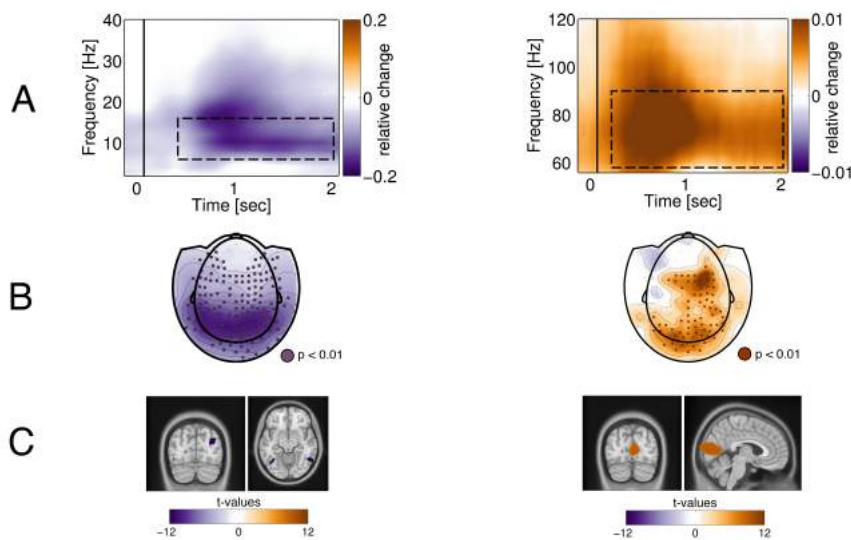
Figure 2: High- and low-frequency activity scales with WM load. A- Time-frequency representations of memory-load-dependent differences in power for low (left) and high (right) frequencies. The color bar indicates difference in oscillatory power (2-back vs. 0-back), with dashed rectangles approximating the time-frequency range contributing to the largest cluster of condition differences. B- Scalp topographical representation of the effect reported in A. Dots highlight the spatial extent of the cluster providing the basis for the rejection of the null-hypothesis, at a p-value of 0.01. C- Source-level representation of condition differences highlighting the strongest (80% of minimum) effects with respect to alpha activity (left) in bilateral fusiform (FF) gyri as well as right intra-parietal sulcus (IPS). In contrast, gamma modulation by WM load was strongest (80% of maximum) in early visual (V1) areas (right graphs). MNI coordinates: right FF [55 -58 -12], right IPS [34 -76 28], V1 [4 -80 8]. Note: alpha activity shows two different loci, whereas the maxima of gamma band activity is predominantly localized in the primary visual cortex.

Alpha-beta and gamma oscillations are inversely related to behavioral performance between and within participants

On average, an increase in WM load resulted in increased RT to the target stimulus.

12

The difference in RT (ΔRT = RT_{2-back}-RT_{0-back}) was on average 131 ms (range 175 to 432 ms; p < 0.0001, t_{82} = 10.05, paired t-test). Figure 3 shows the analysis of the correlation, across subjects, between the behavioral effect and the effect on the time-frequency response. The left panel of Figure 3A illustrates the association between posterior alpha-beta power modulations and RT differences. This indicates that, across participants, stronger alpha power modulations (larger memory-load-dependent decreases) were associated with a larger behavioral penalty (ΔRT), reflecting the increase in WM demands. Participants characterized by stronger alpha-beta decrease with load were also those with a larger RT increase with load. The opposite was observed for gamma activity (Figure 3A right panels). A strong WM-load induced increase in gamma band power was related to an increase in RT differences. Next, we investigated the correlations across trials. The left panels in Figure 3B illustrate the trial-to-trial relationship between alpha-beta oscillations and RT for 0- and 2-back conditions separately. Each line indicates the correlation across trials as a function of time per participant, sorted along the mean reaction time of the respective participant. Prior to the button press there was a positive relationship between alpha-beta power modulation and RT and negative one after response indication. Thus, WM-induced alpha/beta modulations were predictive for individual performance on a trial-by-trial basis. Moreover, this brain-behavior relationship was modulated by WM load (Figure 2B, bottom left panel, p < 0.01 cluster-permutation approach). Similar association differentiating between memory loads was also evident for gamma band activity and RT (Figure 3B, right panels, p < 0.01).

In summary, WM load dependent modulations of alpha-beta and gamma oscillations were found related to behavioral performance both between and within participants. Condition specific differences in alpha-beta and gamma oscillations were characterized by different activation patterns: alpha-beta activity was most pronounced in IPS, whereas maxima of condition differences in gamma band activity were more confined to early visual areas. The correlation between the WM-load dependent gamma response and alpha-beta modulation observed at the sensor-level, combined with the neural sources of the observed effects suggests a cross-frequency interaction between "early" (visual) and "late" (ventral and dorsal) hierarchical levels, which we explored next.

13
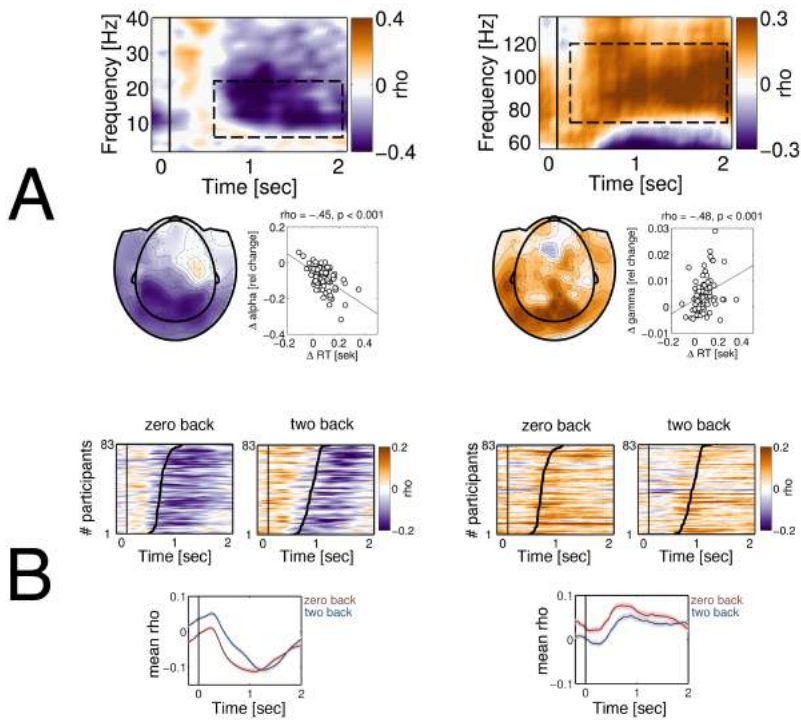
Figure 3: Relationship between neural data and overt performance, and between alpha and gamma power. A) Between-subject relationships. Time-frequency representation of the correlation between RT differences and differences in low- (left) and high- (middle) frequency activity (alpha and RT p < 0.001; gamma and RT p < 0.03; gamma and alpha p < 0.001; cluster-permutation approach). The scatterplots in A are an additional illustration of the respective effects, with each dot corresponding to an individual participant. Time-frequency spectrograms are averaged over occipito-posterior sensors with the following labels: A75, A105, A106, A107, A138, A139, A140, A166, A167, A189, A136, A137, A138, A139, A164, A165. B-Within-subject relationships. Time by participant graphs illustrating the variation of the association between RT and alpha-beta power (left) and RT and gamma power (right). Each line represents a single subject. The color bare indicates correlation coefficients. Participants are sorted according to mean RT time (indicated by the thick black lines). Bottom graphs provide mean correlation over participants with shading indicating +/-1 SEM.

Alpha-beta oscillations in IPS regulate gamma amplitudes in early visual cortex

The results so far suggest an inverse relationship between memory-load-dependent changes in alpha-beta activity on the one hand and the changes in gamma activity on the other. We reconstructed the broadband neural activity at the source locations identified and illustrated in Figure 2. This yielded three virtual sensors per subject, in right IPS, fusiform (FF), and visual (V1) areas. For each participant and brain location, we computed single-trial alpha power averaged between 0.5-2 s and 8-15 Hz. For each of the sets of single-trial alpha power estimates, we performed a median split, dividing the trials into region-specific high
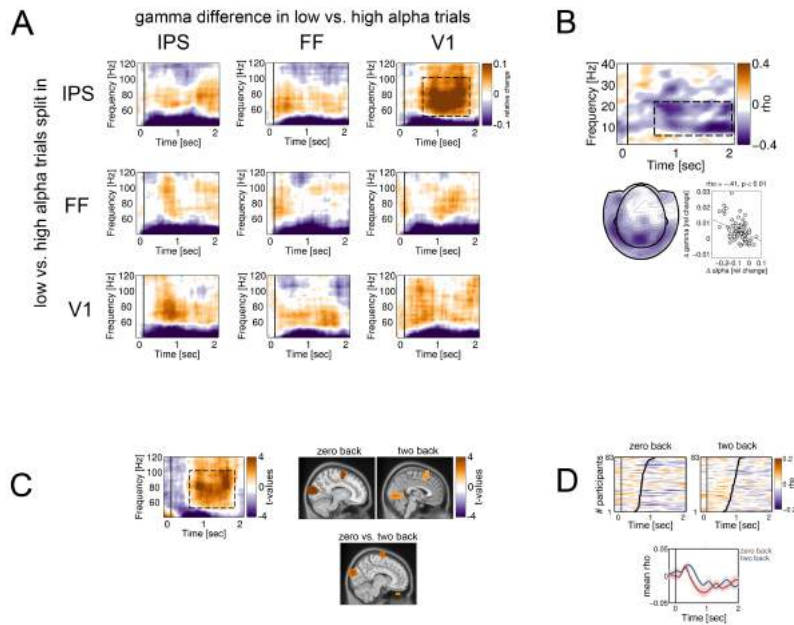
14

and low alpha power trials for each participant. Subsequently, we computed time-frequency representations of power in the gamma range (40-120 Hz) for subsets of trials with low and high alpha power.

The outcome of this analysis is illustrated in Figure 4A. Alpha power decreases in IPS were associated with a sustained relative increase of gamma band activity in V1. That is, on trials with less alpha activity in IPS, gamma amplitude in V1 was higher. This finding was observed only for the IPS-V1 relationships and not for the other possible pairs illustrated in Figure 4A. A control analysis confirmed a robust cross-participant relationship between alpha-beta and gamma activity (60-80Hz) (Figure 4B, p < 0.02 cluster-permutation approach). Whole-brain analysis confirmed that this effect was most pronounced in early visual areas in addition to activation of left motor areas, potentially reflecting the preparation for right-hand button press. Specifically, gamma band activity was reconstructed for high and low IPS alpha trials and subsequently contrasted, resulting in a difference in gamma activity per voxel and per load. Figure 3C illustrates this contrast for 0- and 2-back, respectively as well as their interaction (IPS alpha $_{[high, low]}$ × WM Load $_{[0-back, 2-back]}$). Finally, Figure 4D illustrates this trial-to-trial relationship as a function of time for 0- and 2-back conditions. Each line indicates the correlation across trials as a function of time per participant, sorted along the mean RT of the respective participant. In line with the source-space results, there was significant condition difference between the alpha/gamma correlations in 0- vs. 2-back (Figure 4D, p < 0.02 cluster-permutation approach).

This cross-frequency power relationship is correlative in nature and does not permit conclusions about the potential directionality of effects. These findings suggest a cross-frequency anti-correlation between alpha oscillations in IPS and gamma oscillations in early visual cortex. The extent to which this effect is mediated by top-down (e.g., IPS to V1) or bottom-up (e.g., V1 to IPS) interactions can not be addressed with the analyses reported above, so Granger causality (GC) between the regions of interest derived from that analyses was undertaken.

Dorsal stream exerts top-down control over ventral stream

<u>Conditional</u> GC <u>differentiates</u> direct and mediated influences (Chen et al., 2006; Wen et al., 2013<u>) using</u> a late post-stimulus time window (1 to 2 <u>s)</u> in order to avoid interference from stimulus- and response-locked components. <u>Directed connectivity</u> during <u>WM was</u> probed by <u>a</u> parcellation-based GC analysis (see *Granger causality analysis* <u>method section</u> <u>above).</u> Figure <u>5A</u> confirms the primary condition difference <u>in</u> alpha-beta power in posterior parietal cortex (Figure 5A, left), whereas differences in gamma activity with load were confined mainly to early visual areas (Figure 5A, right). Directed interactions between

cortical structures that survived the time-reversal test are shown in Figure 5B. Dorsal-stream structures such as dorsal visual cortex exhibited directed interactions with ventral-stream structures, such as ventral visual cortex (vVis), medial temporal gyrus (MTG), and area MT as well as visual areas V1, V2/V3 (Figure 5B). This connectivity architecture was evident during both WM conditions. Moreover, this directed communication was predominantly established in the alpha-beta bands (Figure 5B). No GC gamma effects (40+ Hz) were observed. Overall, GC results complement the power-power findings reported above, strengthening the evidence that the dorsal stream exerts top-down control of visual and ventral stream regions via alpha-beta oscillations.
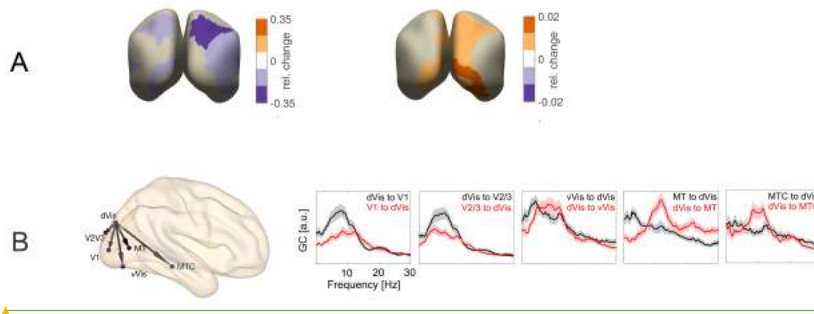
Figure 5: Whole-cortex GC analysis. A- *Source-level representation of cortical parcels illustrating the strongest condition differences with respect to alpha (left) and gamma (right).* ***B-*** *Left panel: Directed connectivity architecture collapsed across WM load. Only connections surviving the time-reversal procedure (see methods) are shown. Right panels: GC spectra (original data) collapsed across WM load averaged over participants per area pair. Red indicates "bottom-up" and black "top-down" directions. Shading depicts SEM. 0-back and 2-back conditions analyzed separately (not shown) showed similar GC spectral profiles.*

Discussion

The present study examined the relationship between low- and high-frequency oscillatory activity during a working memory task. Participants performed an N-back working memory task under low and high load conditions (0-back and 2-back), which allowed us to compare WM-load-dependent stimulus-related changes in oscillatory activity. A large sample of 83 human participants showed modulations of alpha-beta and gamma oscillatory activity that 1) were related to each other across participants, 2) were related to each other across trials within participants, and 3) functionally connected distant brain areas by means of power-power interactions. Moreover, Granger causality analyses showed directed interactions from dorsal-stream parietal areas to ventral-stream areas.

Within- and between-subject relationships between power modulations and reaction time index effortful processing

A key finding of the present report is a robust relationship between the neural and overt performance data, both across subjects and across time within trials (Figure 2B). Cognitive effort was quantified as the increase in RT due to the number of items to be held in memory. This increase in cognitive demand was associated with more decrease in alpha-beta power in IPS and a concurrent increase in gamma power in V1 (Figure 2A). This pattern fits well with the interpretation that decreases in alpha-beta power and increases in gamma power indicate the involvement and overall activation level of task-relevant cortical areas.

Yet, across participants, larger differences in WM-load-dependent power were related to a larger behavioral penalty, i.e. slower RTs with increasing WM load. There was a stronger positive alpha to RT correlation prior to the actual response in the 2-back as compared to the 0-back conditions (Figure 3B). It is conceivable that the parameters of the response-related rebound event-related synchronization (ERS) at alpha-beta frequencies in response to stimulus N-1 correlate with the RT to stimulus N. The magnitude of the ERS indexes the overall readiness of the motor system for a fast response, where higher amplitude is associated with slow responses. Consequently, the observed positive correlation in the 2-back condition at early latencies is increased. Due to the overall slower responses in the 2-back condition, this effect may persist until after onset of the next stimulus. This finding challenges the often tacitly assumed expectation of a positive relationship between oscillatory power modulations and cognitive performance. A number

18

of studies have demonstrated that the amount of alpha-beta power reduction relates to faster RT (Gonzalez Andino et al., 2005; Schoffelen et al., 2005; van Ede et al., 2011; van Ede et al., 2012; Buchholz et al., 2014). A common feature of these studies is the explicit manipulation of attention prior to the behavioral response. Anticipatory attention and/or informative sensory cues might facilitate an anticipatory state, including a decrease in alpha-beta activity. This anticipatory state will result in faster RT to an upcoming target stimulus. One important difference between the present experimental paradigm and the referenced literature is the distinction between stimulus-induced changes in power (induced by task-relevant stimuli that may require a response) and power modulations in oscillatory activity in anticipation of a behaviorally relevant stimulus. Thus, in the results reported here, the increase in gamma/decrease in alpha-beta may reflect increased allocation of local computational resources to process the incoming stimulus and to plan the appropriate response, while having to keep and continuously update two stimuli in memory. Rather than being directly linked to the speed of behavioral responses, oscillatory power modulations may reflect the increased level of simultaneous item maintenance efforts. The reported decrease in alpha activity may reflect the engagement of the visual system in active information processing, with the predominant interplay between ventral and dorsal brain areas potentially reflecting the visual imagery involved in the context of the present task.

Alternatively, instead of neural processes supporting WM that correlate with RT, present findings may reflect motor response processes. In fact, processes related to motor response and WM update processes can co-occur and are not readily dissociable in the present task. However, the strongest condition-specific effects were observed at latencies within the range of the RTs (0.4-1.2 s), thus surrounding the actual motor response. Furthermore, the clear occipito-parietal topography of the correlations and the well-known involvement of these regions during WM tasks suggest that the findings reflect engagement of cortical areas that subserve the more core WM-related processes.

Parietal alpha-beta power fluctuations are related to gamma activity in early visual areas

Extending previous reports showing concurrent stimulus-induced power modulations of alpha and gamma band activity, present findings support a mechanistic view of relationships between neuronal oscillations in different frequency bands and between neuronal oscillations and cognitive performance. Specifically, participants with a stronger

19

WM-load-dependent decrease in alpha-beta power were also characterized by a stronger increase in gamma power. Whereas neuronal generators of gamma activity were confined mainly to early visual areas, the strongest alpha-beta power reduction was predominantly in higher-order parietal areas (Figure 2C). These power-power relationships between low- and high-frequency activity were anatomically specific and are in line with previous reports, highlighting one possible role of parietal brain regions, exerting a top-down control over task-relevant visual cortex (Liu et al., 2014; Michalareas et al., 2016). Furthermore, previous MEG work also considering interactions between gamma and alpha band activity during working memory operations identified the superior temporal gyrus (STG) as a hub region coordinating network activity during maintenance (Park et al., 2011). We observed little engagement of the STG. However, there were several differences in the tasks used. The executive component of the present task involves IPS-V1 interaction, where WM maintenance is typically reflected in frontal to parietal communication (Christophel et al., 2017). Importantly, on a trial-by-trial basis, more alpha power decrease in parietal cortex was associated with a more increase in gamma power in early visual areas (Figure 4), suggesting a direct functional relationship between spatially distant brain areas. Observing a negative correlation in both conditions suggests an involvement of and coordinated interaction between parietal and early visual areas, in line with task requirements. This correlation was stronger for the 0-back than the 2-back condition (Figure 4C). However, the interpretability of this difference is not straightforward. This reflects estimates of both mean power and variance, and on the other hand there was an overall increase in gamma power during the 2-back conditions. Thus, a celling effect on gamma power potentially resulted in a smaller difference between low and high alpha power trials. The extent to which this reflects a behaviourally relevant functional architecture or rather more stimulus-related perceptual processes remains to be demonstrated. On the basis of this functional power to power relationship between IPS alpha and V1 gamma, we next examined the effective communication between these nodes.

Dorsal-stream-to-ventral-stream interactions at alpha-beta frequencies

GC analysis indicated a unidirectional relationship from dorsal visual to ventral visual areas relying on alpha-beta frequencies (Figure 5B), with no clear GC spectral peak at gamma frequencies. Early visual areas were receiving input from dorsal areas primarily at

alpha-beta frequencies (Figure 4A). These results are partially in line with reports from human and animal research, demonstrating that feedback interactions operate in the intermediate alpha-beta range (Saalmann et al., 2012; van Kerkoerle et al., 2014; Bastos et al., 2015; Michalareas et al., 2016; Popov et al., 2017). Previous literature suggests that, for perceptual tasks strongly engaging the dorsal stream, dorsal regions affect mid-level ventral-stream regions more than early visual areas (Michalareas et al., 2016). Present findings are consistent with this, demonstrating that, during high WM load, dorsal alpha activity is a mechanism of top-down control over ventral regions, despite an experimental arrangement strongly engaging the ventral stream (e.g., face identity).

Conclusions
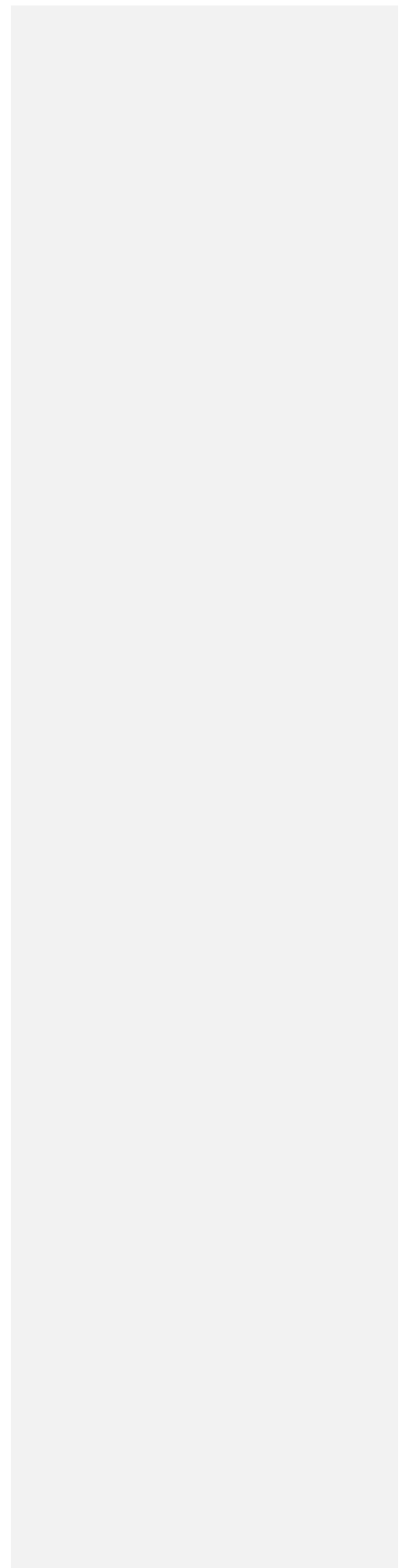
In summary, the present study analyzed publicly available MEG data from 83 participants while they performed an N-back task. We investigated the relationship between neural activity (low- and high frequency oscillations) and overt performance (task condition and RT). Increased working memory demands resulted in alpha-beta and gamma power modulations in early visual cortex and brain regions in the dorsal and ventral visual streams. Robust cross-frequency power-to-power interactions between these brain areas and between alpha-beta and gamma activity during WM scaled with WM demands. Granger causality interactions were most prominent in the alpha band, from dorsal stream to ventral stream areas. Overall, these data confirm earlier findings and provide additional support for the notion that fluctuations in band-limited neural activity reflect behaviorally relevant local and inter-regional neural processing. In addition, this work shows the utility of employing publicly available, task-based MEG data for exploratory and confirmatory purposes.

Acknowledgments

I

I

References

Adrian ED, Matthews BHC (1934) The Berger rhythm: potential changes from the occipital lobes in man. Brain 57:355-384.

Allen EA, Liu J, Kiehl KA, Gelernter J, Pearlson GD, Perrone-Bizzozero NI, Calhoun VD (2011) Components of cross-frequency modulation in health and disease. Frontiers in systems neuroscience 5:59.

Axmacher N, Henseler MM, Jensen O, Weinreich I, Elger CE, Fell J (2010) Cross-frequency coupling supports multi-item working memory in the human hippocampus. Proceedings of the National Academy of Sciences of the United States of America 107:3228-3233.

Bastos AM, Vezoli J, Bosman CA, Schoffelen JM, Oostenveld R, Dowdall JR, De Weerd P, Kennedy H, Fries P (2015) Visual Areas Exert Feedforward and Feedback Influences through Distinct Frequency Channels. Neuron 85:390-401.

Bauer M, Stenner MP, Friston KJ, Dolan RJ (2014) Attentional modulation of alpha/beta and gamma oscillations reflect functionally distinct processes. The Journal of neuroscience : the official journal of the Society for Neuroscience 34:16117-16125.

Berman JI, Liu S, Bloy L, Blaskey L, Roberts TP, Edgar JC (2015) Alpha-to-gamma phase-amplitude coupling methods and application to autism spectrum disorder. Brain Connect 5:80-90.

Buchholz VN, Jensen O, Medendorp WP (2014) Different roles of alpha and beta band oscillations in anticipatory sensorimotor gating. Frontiers in human neuroscience 8:446.

Buzsaki G, Draguhn A (2004) Neuronal oscillations in cortical networks. Science 304:1926-1929.

Canolty RT, Knight RT (2010) The functional role of cross-frequency coupling. Trends in cognitive sciences 14:506-515.

Chen Y, Bressler SL, Ding M (2006) Frequency decomposition of conditional Granger causality and application to multivariate neural field potential data. Journal of neuroscience methods 150:228-237.

Christophel TB, Klink PC, Spitzer B, Roelfsema PR, Haynes JD (2017) The Distributed Nature of Working Memory. Trends in cognitive sciences 21:111-124.

Cooper NR, Croft RJ, Dominey SJ, Burgess AP, Gruzelier JH (2003) Paradox lost? Exploring the role of alpha oscillations during externally vs. internally directed attention and the implications for idling and inhibition hypotheses. International journal of psychophysiology : official journal of the International Organization of Psychophysiology 47:65-74.

de Lange FP, Jensen O, Bauer M, Toni I (2008) Interactions between posterior gamma and frontal alpha/beta oscillations during imagined actions. Frontiers in human neuroscience 2:7.

Dhamala M, Rangarajan G, Ding M (2008) Estimating Granger causality from fourier and wavelet transforms of time series data. Phys Rev Lett 100:018701.

Ding M, Chen Y, Bressler S (2006) Granger Causality: Basic Theory and Application to Neuroscience. In: Handbook of Time Series Analysis, (Schelter B, Winterhalder M, Timmer J, eds), pp 451-474: Wiley-VCH Verlage.

Florin E, Baillet S (2015) The brain's resting-state activity is shaped by synchronized cross-frequency coupling of neural oscillations. NeuroImage 111:26-35.

1   Foxe JJ, Simpson GV, Ahlfors SP (1998) Parieto-occipital approximately 10 Hz activity
2   reflects anticipatory state of visual attention mechanisms. Neuroreport 9:3929-3933.
3   Fries P (2005) A mechanism for cognitive dynamics: neuronal communication through
4   neuronal coherence. Trends in cognitive sciences 9:474-480.
5   Gevins A, Smith ME, McEvoy L, Yu D (1997) High-resolution EEG mapping of cortical
6   activation related to working memory: effects of task difficulty, type of processing,
7   and practice. Cerebral cortex 7:374-385.
8   Geweke J (1982) Measurment of linear dependence and feedback between multiple time
9   series. J Am Stat Assoc 77:304-313.
10   Glasser MF, Coalson TS, Robinson EC, Hacker CD, Harwell J, Yacoub E, Ugurbil K,
11   Andersson J, Beckmann CF, Jenkinson M, Smith SM, Van Essen DC (2016) A multi-
12   modal parcellation of human cerebral cortex. Nature 536:171-178.
13   Gonzalez Andino SL, Michel CM, Thut G, Landis T, Grave de Peralta R (2005) Prediction of
14   response speed by anticipatory high-frequency (gamma band) oscillations in the
15   human brain. Human brain mapping 24:50-58.
16   Granger CWJ (1969) Investigating Causal Relations by Econometric Models and Cross-
17   spectral Methods. Econometrica 37:424-438.
18   Gross J, Kujala J, Hamalainen M, Timmermann L, Schnitzler A, Salmelin R (2001) Dynamic
19   imaging of coherent sources: Studying neural interactions in the human brain.
20   Proceedings of the National Academy of Sciences of the United States of America
21   98:694-699.
22   Haegens S, Handel BF, Jensen O (2011) Top-down controlled alpha band activity in
23   somatosensory areas determines behavioral performance in a discrimination task.
24   The Journal of neuroscience : the official journal of the Society for Neuroscience
25   31:5197-5204.
26   Haegens S, Osipova D, Oostenveld R, Jensen O (2010) Somatosensory working memory
27   performance in humans depends on both engagement and disengagement of regions
28   in a distributed network. Human brain mapping 31:26-35.
29   Haufe S, Nikulin VV, Muller KR, Nolte G (2013) A critical assessment of connectivity
30   measures for EEG data: a simulation study. NeuroImage 64:120-133.
31   Hoogenboom N, Schoffelen JM, Oostenveld R, Fries P (2010) Visually induced gamma-band
32   activity predicts speed of change detection in humans. NeuroImage 51:1162-1167.
33   Hoogenboom N, Schoffelen JM, Oostenveld R, Parkes LM, Fries P (2006) Localizing human
34   visual gamma-band activity in frequency, time and space. NeuroImage 29:764-773.
35   Jensen O, Colgin LL (2007) Cross-frequency coupling between neuronal oscillations. Trends
36   in cognitive sciences 11:267-269.
37   Jensen O, Mazaheri A (2010) Shaping functional architecture by oscillatory alpha activity:
38   gating by inhibition. Frontiers in human neuroscience 4:186.
39   Jung TP, Makeig S, McKeown MJ, Bell AJ, Lee TW, Sejnowski TJ (2001) Imaging Brain
40   Dynamics Using Independent Component Analysis. Proceedings of the IEEE Institute
41   of Electrical and Electronics Engineers 89:1107-1122.
42   Kaminski M, Ding M, Truccolo WA, Bressler SL (2001) Evaluating causal relations in neural
43   systems: granger causality, directed transfer function and statistical assessment of
44   significance. Biol Cybern 85:145-157.
45   Kirihara K, Rissling AJ, Swerdlow NR, Braff DL, Light GA (2012) Hierarchical organization of
46   gamma and theta oscillatory dynamics in schizophrenia. Biological psychiatry 71:873-
47   880.
48   Klimesch W, Sauseng P, Hanslmayr S (2007) EEG alpha oscillations: the inhibition-timing
49   hypothesis. Brain research reviews 53:63-88.
50   Kujala J, Jung J, Bouvard S, Lecaignard F, Lothe A, Bouet R, Ciumas C, Ryvlin P, Jerbi K
51   (2015) Gamma oscillations in V1 are correlated with GABA(A) receptor density: A

multi-modal MEG and Flumazenil-PET study. Sci Rep 5:16347.

Leszczynski M, Fell J, Axmacher N (2015) Rhythmic Working Memory Activation in the Human Hippocampus. Cell Rep 13:1272-1282.

Lisman JE, Jensen O (2013) The theta-gamma neural code. Neuron 77:1002-1016.

Maris E, Oostenveld R (2007) Nonparametric statistical testing of EEG- and MEG-data. Journal of neuroscience methods 164:177-190.

Marshall TR, Bergmann TO, Jensen O (2015a) Frontoparietal Structural Connectivity Mediates the Top-Down Control of Neuronal Synchronization Associated with Selective Attention. PLoS biology 13:e1002272.

Marshall TR, O'Shea J, Jensen O, Bergmann TO (2015b) Frontal eye fields control attentional modulation of alpha and gamma oscillations in contralateral occipitoparietal cortex. The Journal of neuroscience : the official journal of the Society for Neuroscience 35:1638-1647.

Mazaheri A, van Schouwenburg MR, Dimitrijevic A, Denys D, Cools R, Jensen O (2014) Region-specific modulations in oscillatory alpha activity serve to facilitate processing in the visual and auditory modalities. NeuroImage 87:356-362.

Michalareas G, Vezoli J, van Pelt S, Schoffelen JM, Kennedy H, Fries P (2016) Alpha-Beta and Gamma Rhythms Subserve Feedback and Feedforward Influences among Human Visual Cortical Areas. Neuron.

Miskovic V, Moscovitch DA, Santesso DL, McCabe RE, Antony MM, Schmidt LA (2011) Changes in EEG cross-frequency coupling during cognitive behavioral therapy for social anxiety disorder. Psychol Sci 22:507-516.

Mitra PP, Pesaran B (1999) Analysis of dynamic brain imaging data. Biophysical journal 76:691-708.

Muthukumaraswamy SD, Singh KD (2013) Visual gamma oscillations: the effects of stimulus type, visual field coverage and stimulus motion on MEG and EEG recordings. NeuroImage 69:223-230.

Nolte G (2003) The magnetic lead field theorem in the quasi-static approximation and its use for magnetoencephalography forward calculation in realistic volume conductors. Physics in medicine and biology 48:3637-3652.

Oldfield RC (1971) The assessment and analysis of handedness: the Edinburgh inventory. Neuropsychologia 9:97-113.

Oostenveld R, Fries P, Maris E, Schoffelen JM (2011) FieldTrip: Open source software for advanced analysis of MEG, EEG, and invasive electrophysiological data. Computational intelligence and neuroscience 2011:156869.

Park H, Kang E, Kang H, Kim JS, Jensen O, Chung CK, Lee DS (2011) Cross-frequency power correlations reveal the right superior temporal gyrus as a hub region during working memory maintenance. Brain Connect 1:460-472.

Park H, Lee DS, Kang E, Kang H, Hahm J, Kim JS, Chung CK, Jiang H, Gross J, Jensen O (2016) Formation of visual memories controlled by gamma power phase-locked to alpha oscillations. Sci Rep 6:28092.

Perry G, Hamandi K, Brindley LM, Muthukumaraswamy SD, Singh KD (2013) The properties of induced gamma oscillations in human visual cortex show individual variability in their dependence on stimulus size. NeuroImage 68:83-92.

Popov T, Popova P (2015) Same clock, different time read-out: Spontaneous brain oscillations and their relationship to deficient coding of cognitive content. NeuroImage 119:316-324.

Popov T, Kastner S, Jensen O (2017) FEF-Controlled Alpha Delay Activity Precedes Stimulus-Induced Gamma-Band Activity in Visual Cortex. The Journal of neuroscience : the official journal of the Society for Neuroscience 37:4117-4127.

Roux F, Uhlhaas PJ (2014) Working memory and neural oscillations: alpha-gamma versus

theta-gamma codes for distinct WM information? Trends in cognitive sciences 18:16-25.

Roux F, Wibral M, Mohr HM, Singer W, Uhlhaas PJ (2012) Gamma-band activity in human prefrontal cortex codes for the number of relevant items maintained in working memory. The Journal of neuroscience : the official journal of the Society for Neuroscience 32:12411-12420.

Saalmann YB, Pinsk MA, Wang L, Li X, Kastner S (2012) The pulvinar regulates information transmission between cortical areas based on attention demands. Science 337:753-756.

Schoffelen JM, Oostenveld R, Fries P (2005) Neuronal coherence as a mechanism of effective corticospinal interaction. Science 308:111-113.

Schoffelen JM, Hulten A, Lam N, Marquand AF, Udden J, Hagoort P (2017) Frequency-specific directed interactions in the human brain network for language. Proceedings of the National Academy of Sciences of the United States of America 114:8083-8088.

Spaak E, Bonnefond M, Maier A, Leopold DA, Jensen O (2012) Layer-specific entrainment of gamma-band neural activity by the alpha rhythm in monkey visual cortex. Current biology : CB 22:2313-2318.

Staresina BP, Bergmann TO, Bonnefond M, van der Meij R, Jensen O, Deuker L, Elger CE, Axmacher N, Fell J (2015) Hierarchical nesting of slow oscillations, spindles and ripples in the human hippocampus during sleep. Nat Neurosci 18:1679-1686.

Staudigl T, Hanslmayr S (2013) Theta oscillations at encoding mediate the context-dependent nature of human episodic memory. Current biology : CB 23:1101-1106.

Swettenham JB, Muthukumaraswamy SD, Singh KD (2009) Spectral properties of induced and evoked gamma oscillations in human early visual cortex to moving and stationary stimuli. Journal of neurophysiology 102:1241-1253.

Tallon-Baudry C, Bertrand O (1999) Oscillatory gamma activity in humans and its role in object representation. Trends in cognitive sciences 3:151-162.

Tallon-Baudry C, Bertrand O, Peronnet F, Pernier J (1998) Induced gamma-band activity during the delay of a visual short-term memory task in humans. The Journal of neuroscience : the official journal of the Society for Neuroscience 18:4244-4254.

Tort AB, Komorowski R, Eichenbaum H, Kopell N (2010) Measuring phase-amplitude coupling between neuronal oscillations of different frequencies. Journal of neurophysiology 104:1195-1210.

Tort AB, Komorowski RW, Manns JR, Kopell NJ, Eichenbaum H (2009) Theta-gamma coupling increases during the learning of item-context associations. Proceedings of the National Academy of Sciences of the United States of America 106:20942-20947.

Tort AB, Kramer MA, Thorn C, Gibson DJ, Kubota Y, Graybiel AM, Kopell NJ (2008) Dynamic cross-frequency couplings of local field potential oscillations in rat striatum and hippocampus during performance of a T-maze task. Proceedings of the National Academy of Sciences of the United States of America 105:20517-20522.

van Ede F, de Lange FP, Maris E (2012) Attentional cues affect accuracy and reaction time via different cognitive and neural processes. The Journal of neuroscience : the official journal of the Society for Neuroscience 32:10408-10412.

van Ede F, Szebenyi S, Maris E (2014) Attentional modulations of somatosensory alpha, beta and gamma oscillations dissociate between anticipation and stimulus processing. NeuroImage 97:134-141.

van Ede F, de Lange F, Jensen O, Maris E (2011) Orienting attention to an upcoming tactile event involves a spatially and temporally specific modulation of sensorimotor alpha-and beta-band oscillations. The Journal of neuroscience : the official journal of the Society for Neuroscience 31:2016-2024.

van Kerkoerle T, Self MW, Dagnino B, Gariel-Mathis MA, Poort J, van der Togt C,

Roelfsema PR (2014) Alpha and gamma oscillations characterize feedback and feedforward processing in monkey visual cortex. Proceedings of the National Academy of Sciences of the United States of America 111:14332-14341.

Van Veen BD, van Drongelen W, Yuchtman M, Suzuki A (1997) Localization of brain electrical activity via linearly constrained minimum variance spatial filtering. IEEE transactions on bio-medical engineering 44:867-880.

van Wijk BC, Beudel M, Jha A, Oswal A, Foltynie T, Hariz MI, Limousin P, Zrinzo L, Aziz TZ, Green AL, Brown P, Litvak V (2016) Subthalamic nucleus phase-amplitude coupling correlates with motor impairment in Parkinson's disease. Clin Neurophysiol 127:2010-2019.

Wang L, Hagoort P, Jensen O (2017) Language Prediction Is Reflected by Coupling between Frontal Gamma and Posterior Alpha Oscillations. Journal of cognitive neuroscience:1-16.

Weisz N, Hartmann T, Muller N, Lorenz I, Obleser J (2011) Alpha rhythms in audition: cognitive and clinical perspectives. Frontiers in psychology 2:73.

Wen X, Rangarajan G, Ding M (2013) Multivariate Granger causality: an estimation framework based on factorization of the spectral density matrix. Philosophical transactions Series A, Mathematical, physical, and engineering sciences 371:20110610.

Whittingstall K, Logothetis NK (2009) Frequency-band coupling in surface EEG reflects spiking activity in monkey visual cortex. Neuron 64:281-289.

Wilson GT (1972) The factorization of matrical spectral densities. SIAM J Appl Math 23:420-426.

Winkler I, Haufe S, Porbadnigk AK, Muller KR, Dahne S (2015) Identifying Granger causal relationships between neural power dynamics and variables of interest. NeuroImage 111:489-504.